Atmospheric CO_2 uptake by a coastal upwelling system

Burke Hales
College of Oceanic and Atmospheric Sciences, Oregon State University, Corvallis, Oregon, USA

Taro Takahashi
Lamont-Doherty Earth Observatory of Columbia University, Palisades, New York, USA

Leah Bandstra
College of Oceanic and Atmospheric Sciences, Oregon State University, Corvallis, Oregon, USA

Received 5 May 2004; revised 24 September 2004; accepted 22 November 2004; published 2 February 2005.

[1] A biological pump for transferring atmospheric CO_2 to deep ocean regimes has been identified in the upwelling zone of the U.S. Pacific coast off Oregon using high-resolution measurements of P_{CO2} and nutrient concentrations that were made in May through August 2001. Surface water over most of the shelf was a strong sink for atmospheric CO_2, while a narrow nearshore strip was an intense source. The dominance of the low-CO_2 waters over the shelf area makes the region a net sink during upwelling season. This is due to (1) upwelled water that carries abundant preformed nutrients, (2) complete photosynthetic uptake of these excess nutrients and a stoichiometric proportion of CO_2, and (3) moderate warming of upwelled waters. If the remaining North Pacific's eastern boundary area is assumed to have similar conditions, this area should represent a sink of atmospheric CO_2 that is 5% of the annual North Pacific CO_2 uptake, and roughly equivalent to the North Pacific's uptake in the summer season. By mid-August, P_{CO2} in subsurface waters increased 20–60%, corresponding to a 1.0–2.3% TCO_2 increase, due to respiration of settling biogenic debris. This water would be transported off the shelf to depth by winter downwelling flow, providing an important mechanism for sequestering atmospheric CO_2 into the oceans' interior.

Citation: Hales, B., T. Takahashi, and L. Bandstra (2005), Atmospheric CO_2 uptake by a coastal upwelling system, *Global Biogeochem. Cycles*, *19*, GB1009, doi:10.1029/2004GB002295.

1. Introduction and Background

[2] The summertime Oregon coastal ocean is a region of strong upwelling. Prevailing equatorward alongshore winds drive net surface Ekman flow offshore from the coast, creating a divergence along the coastline which draws dense, nutrient-rich subsurface waters across the upward-sloping bottom contours toward shore [*Allen et al.*, 1995; *Federiuk and Allen*, 1995; *Huyer et al.*, 1978; *Lentz*, 1992; *Huyer et al.*, 1979; *Strub et al.*, 1987a, 1987b]. Cross-shelf transport inshore of the shelf break is dominated by this process. *Lentz* [1992] showed that lateral mixing via eddy diffusion is negligible relative to the cross-shelf Ekman/upwelling advective transport in the heat budget. While there are numerous examples of eddies and filaments detaching from the shelf break front and moving into the open ocean [e.g., *Barth et al.*, 2002, 2000], movement of such features in the opposite direction across the shelf break is rare due to potential vorticity conservation restrictions imposed by the compression of the water column by the upward sloping seafloor. This effectively eliminates the contribution of large-scale eddy and current-meander processes to lateral mixing in the coastal ocean, and an upper-bound estimate of the horizontal mixing coefficient (or eddy diffusivity) there is 1 $m^2\ s^{-1}$ (J. Barth, Oregon State University, personal communication, 2004). Although cross-shelf velocities driven by Ekman transport and coastal divergence are low, on the order of kilometers per day [*Lentz*, 1992; *Perlin et al.*, 2005], cross-shelf advective transport is orders of magnitude faster than cross-shelf transport by mixing. Timescales of cross-shelf advective transport are measured in tens of days, while timescales of random cross-shelf mixing at the rate given above are measured in thousands of days. (The mixing timescale is estimated simply from $t = L^2/(2*Kh)$, where L is the width of the shelf and Kh is the horizontal mixing coefficient. For conservative estimates of Kh = 1 m^2/s, L = 30 km, t > 5000 days.) The Columbia River plume flows southward along the outer edge of the shelf break at this time of year, providing a boundary between the coastal and open ocean. These physical characteristics of the system combine to minimize the effects of the surface open ocean on shelf waters during upwelling season.

0886-6236/05/2004GB002295$12.00

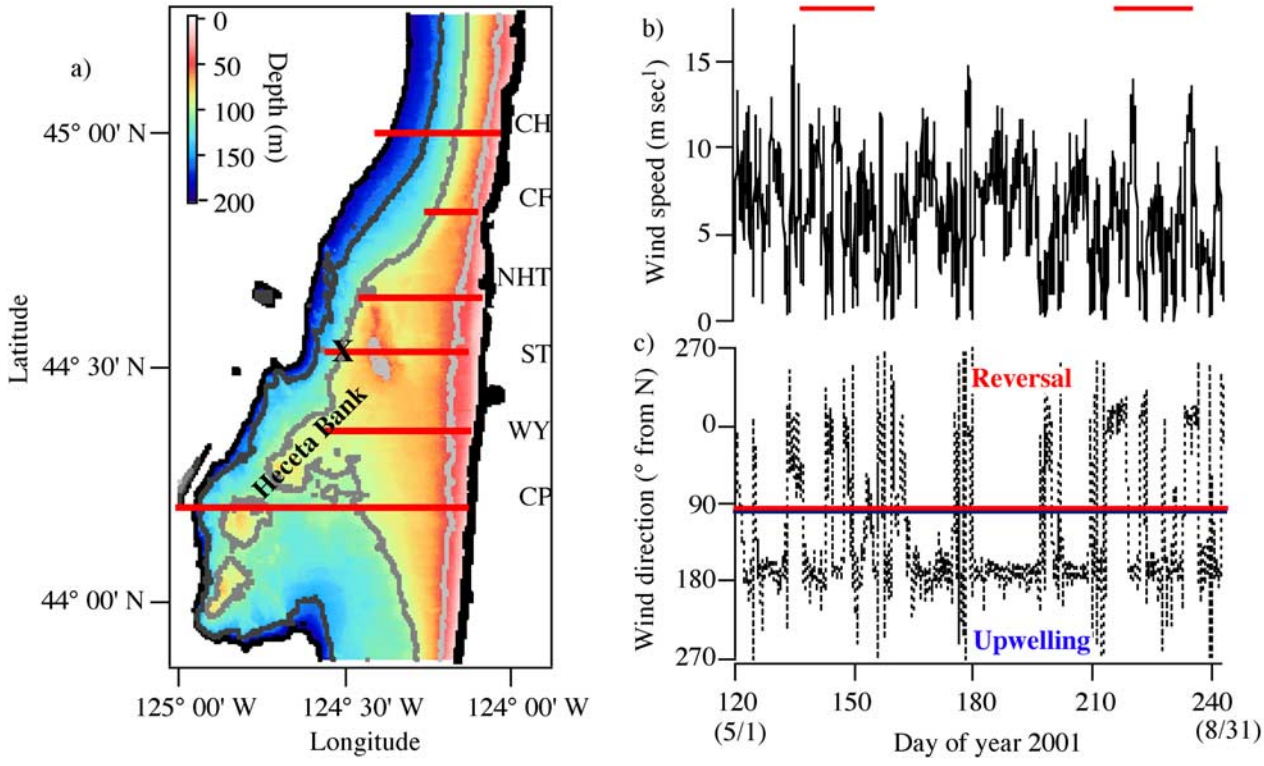

Figure 1. (a) Study area, showing locations of the cross-shelf surveys as red horizontal bars (CH, Cascade Head; CF, Cape Foulweather; NHT, Newport; ST, Stonewall Bank; WY, Waldport-Yachats; CP, Cape Perpetua). Bathymetry is shown as color shading and corresponding contours at 50 m intervals from 0 to 200 m. The black cross on the ST line denotes the position of the meteorological buoy NDBC 46050 where the wind data in Figures 1b and 1c were collected. (b) Wind speed and (c) direction for the May–August upwelling season of 2001, with the durations of the two research cruises overlain as solid horizontal bars in Figure 1b. Predominantly southward winds (direction $\approx 180°$) drive upwelling, while predominantly northward winds (direction $\approx 0°$) result in reversal events.

[3] Photosynthesis by coastal phytoplankton is sufficiently fast [*Dugdale et al.*, 1990] that upwelled nutrients are depleted over the seaward edge of the shelf [*Kokkinakis and Wheeler*, 1987] (see also Hales et al., Irreversible nitrate fluxes due to turbulent mixing in a coastal upwelling system submitted to *Journal of Geophysical Research*, 2004) (hereinafter referred to as Hales et al., submitted manuscript, 2004). This, in conjunction with the origin of the upwelled waters in the upper thermocline of the North Pacific, results in a dynamic range of nutrient concentrations approaching that seen across the world ocean. This variability is compressed in the <200 m depth and <100 km width spatial scale of the ocean margin. Changes in the concentrations of total dissolved CO_2 (T_{CO2}) and nutrients observed in surface waters are consistent with the photosynthetic stoichiometry of *Redfield et al.* [1963]. As a result, CO_2 partial pressure (P_{CO2}) is expected to show even greater variability, given a tenfold or greater amplification of P_{CO2} changes relative to T_{CO2} because of the Revelle factor [*Broecker and Peng*, 1980]. Despite this large, short-length-scale variability, there have been no high-resolution spatial surveys of the chemistry of these shelf waters, and few studies of the CO_2 chemistry of shelf waters at any resolution.

[4] A number of other studies have recently examined the role of processes unique to ocean margins in exporting CO_2 to the deep ocean via the gravitational settling of photosynthetic products from surface waters to depths below seasonally stratified layers [*Thomas et al.*, 2004; *Chen et al.*, 2004; *Tsunogai et al.*, 1999; *Yool and Fasham*, 2001; *DeGrandpre et al.*, 2002; A. Bianchi et al., Vertical stratification and air-sea CO_2 fluxes in the Patagonian shelf, submitted to *Journal of Geophysical Research*, 2004]. In contrast, we present data showing that wind-driven upwelling margins can also take up atmospheric CO_2, and suggest a mechanism whereby other margins supplied by water with abundant preformed nutrients can be a sink as well.

2. Setting and Methods

[5] During the Coastal Ocean Processes (CoOP; http://www.skio.peachnet.edu/research/coop) sponsored Coastal Ocean Advances in Shelf Transport (COAST; http://damp.oce.orst.edu/coast) program, we performed high spatial resolution measurements of nutrient and carbonate chemistry in the upper 200 m of the water column off the Oregon coast in summer 2001. Six cross-shelf sections (Figure 1a) were selected to study physical and biogeochemical pro-

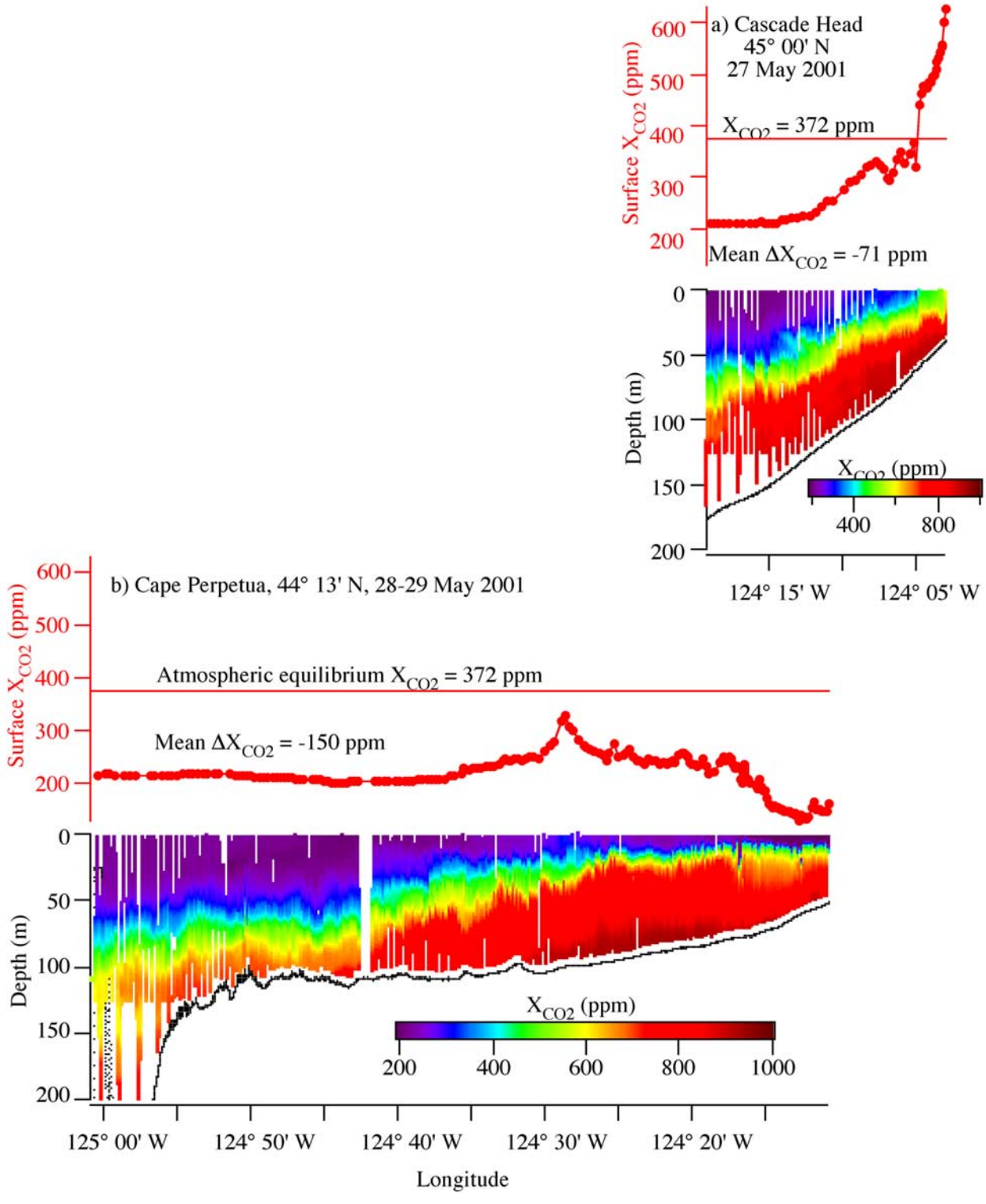

Figure 2. Cross-shelf distributions of X_{CO2} at in situ water temperature at (a) Cascade Head (45°00′N) and (b) Cape Perpetua (44°13′N) in May 2001.

cesses along a gradient of increasing shelf width and bathymetric complexity. The northernmost section (at Cascade Head, 45°00′N) spans a narrow shelf with uniform, near-parallel depth contours. The southernmost (at Cape Perpetua, 44°13′N) spans Heceta Bank, a broad seaward protrusion including numerous bathymetric highs and lows. Some sections were measured repeatedly in May and August 2001. Wind-forcing (Figures 1b and 1c) was typical

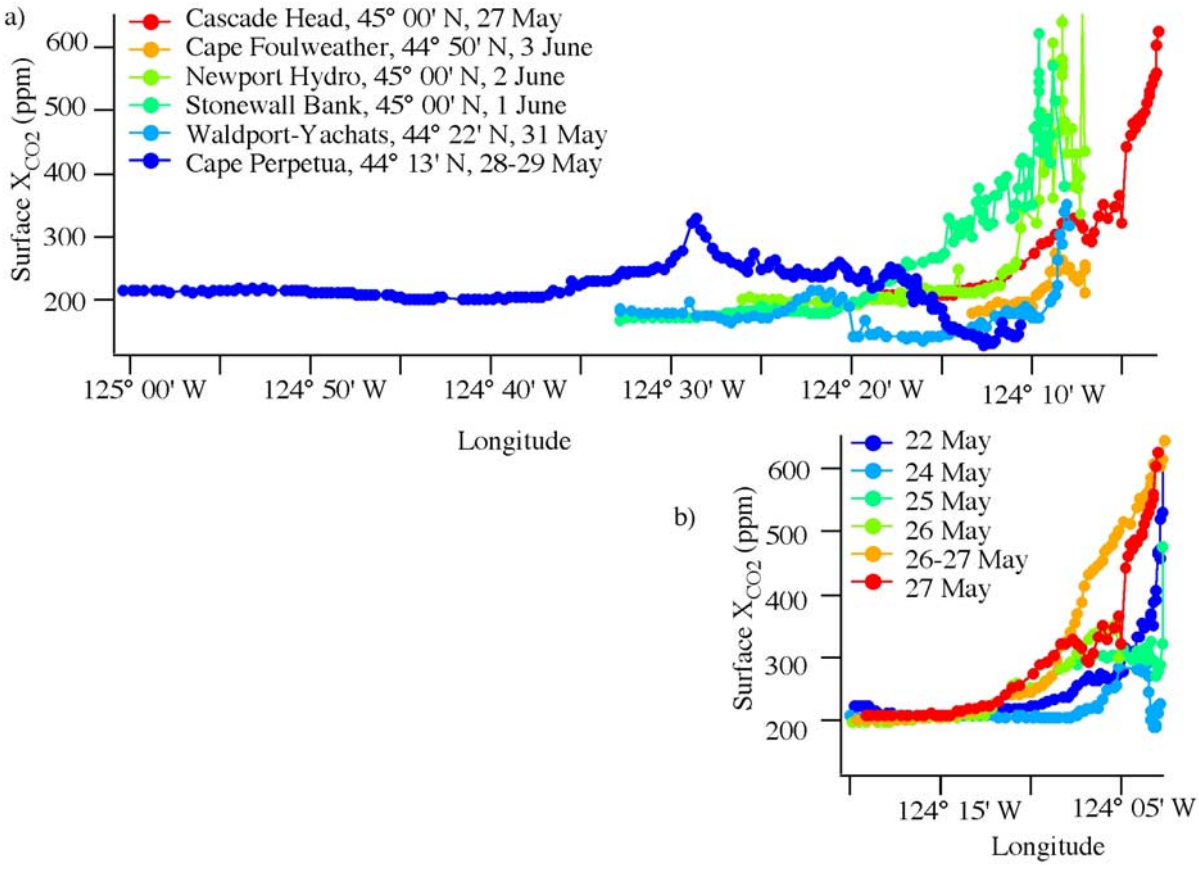

Figure 3. Cross-shelf distributions of surface-water X_{CO2} for (a) all transects shown in Figure 1a for the time period spanning 27 May to 2 June and (b) a time period spanning 22–27 May at the Cascade Head transect.

of summer upwelling, with predominantly upwelling-favorable equatorward winds throughout the season. These conditions were punctuated by several brief reversal events defined by poleward winds with speeds approximately equivalent to those seen during typical conditions. The frequency distribution of wind direction (not shown) is bimodal, with a strong maximum of north-northwest winds, and a much smaller secondary maximum of south-southwest winds. Wind speed frequency distribution is unimodal, with a maximum at about 6 m s^{-1}. Wind events with more westerly or easterly character are extremely rare, and wind speed is not significantly correlated with wind direction.

[6] To do this work, we developed a system that continuously pumped seawater from a towed, winch-controlled, "sled" back to the shipboard laboratory for high-speed chemical analyses, while automatically and continuously profiling between the sea surface and seafloor. In the laboratory, we operated fast-response analytical systems measuring nutrient concentrations [*Hales et al.*, 2004a] and P_{CO2} [*Hales et al.*, 2004b] (expressed hereinafter as X_{CO2}, the mole-fraction or mixing ratio of CO_2 in dry air) at ≈1 Hz frequencies. The sled carried sensors for in situ measurement of depth, temperature, salinity, oxygen concentration, and other bio-optical and operational parameters. Shipboard measurement times were phase-shifted for analytical and sampling lag times and synchronized with the in situ data, following the approach of *Hales and Takahashi* [2002, 2004]. Vertical profiling rates of 0.3 m s^{-1} and ship speeds of 1–2 m s^{-1} resulted in vertical resolution of ∼1 m and horizontal resolution of 200–2000 m for water depths of 30–200 m.

3. Results

[7] X_{CO2} distributions at the northernmost site on 27 May 2001 (Figure 2a) show near-1000 ppm water along the bottom that encroaches upward toward the nearshore. The effect of upwelling on the surface water is clear at the shoreward end of the section, where surface X_{CO2} (Figure 2a, top panel) exceeds 600 ppm, far above the atmospheric-equilibrium X_{CO2} of 372 ± 3 ppm (GLOBALVIEW-CO2: Cooperative Atmospheric Data Integration Project–Carbon Dioxide, 2003, available at www.cmdl.noaa.gov/ccg/globalview/co2; file ref_mbl_mtx.co2). The area of this water's exposure to the surface, however, is quite narrow, as surface-water

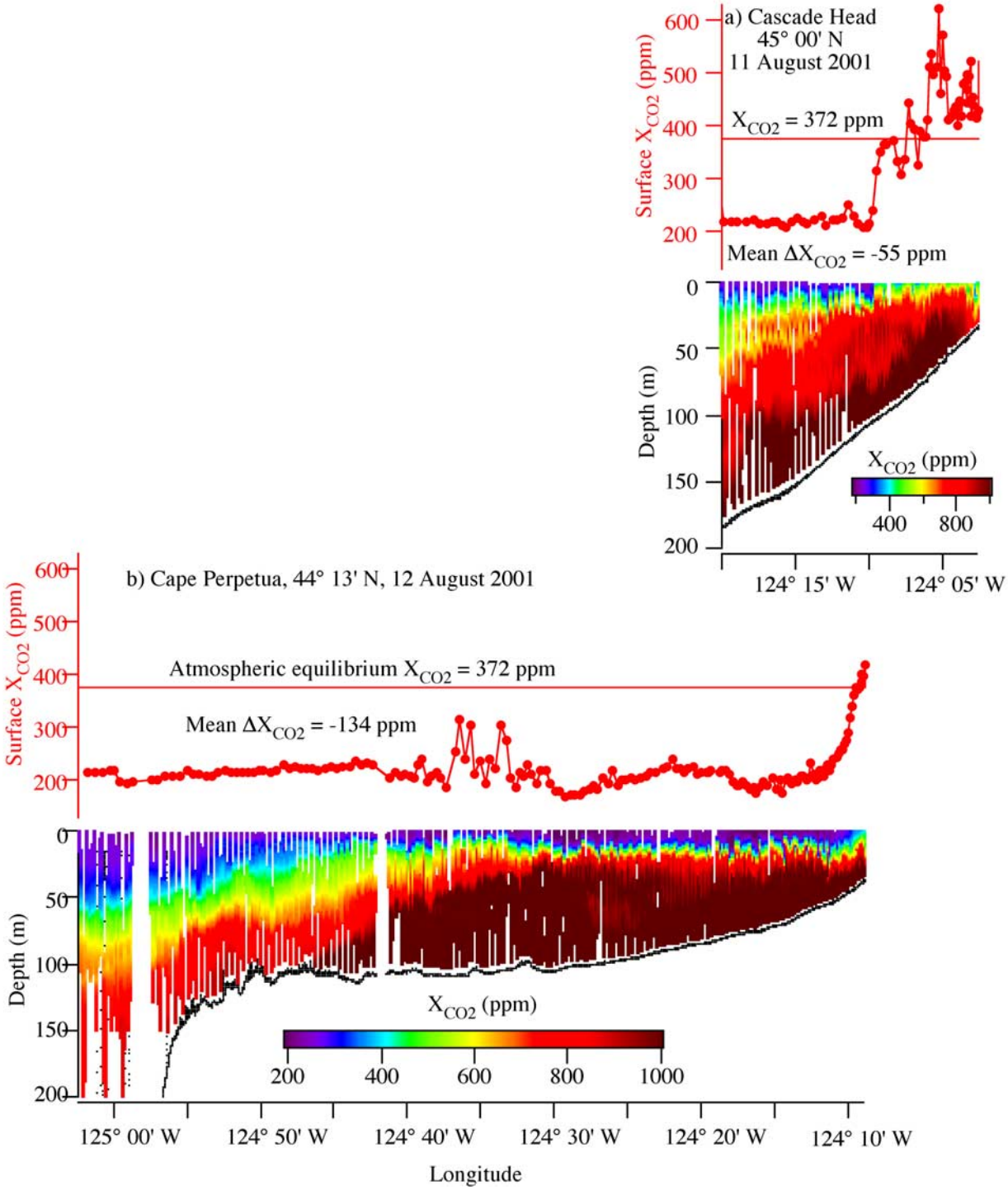

Figure 4. Cross-shelf distributions of X_{CO2} at (a) Cascade Head and (b) Cape Perpetua, as in Figures 2a and 2b, during 11–12 August 2001.

X_{CO2} values rapidly decrease seaward to values as low as 200 ppm. The longitudinally (E-W)-weighted cross-shelf average surface X_{CO2} is 301 ppm, corresponding to a sea-air difference (ΔX_{CO2}) of −71 ppm and indicating a net transfer of CO_2 from atmosphere to ocean. The extent of this undersaturation is even more striking at the Cape Perpetua site. While near-bottom waters have high X_{CO2} as seen at the northern site (Figure 2b, bottom panel), surface waters (Figure 2b, top panel) are strongly undersaturated with respect to the atmosphere across the entire section, with values as low as 150 ppm and an average ΔX_{CO2} of −153 ppm.

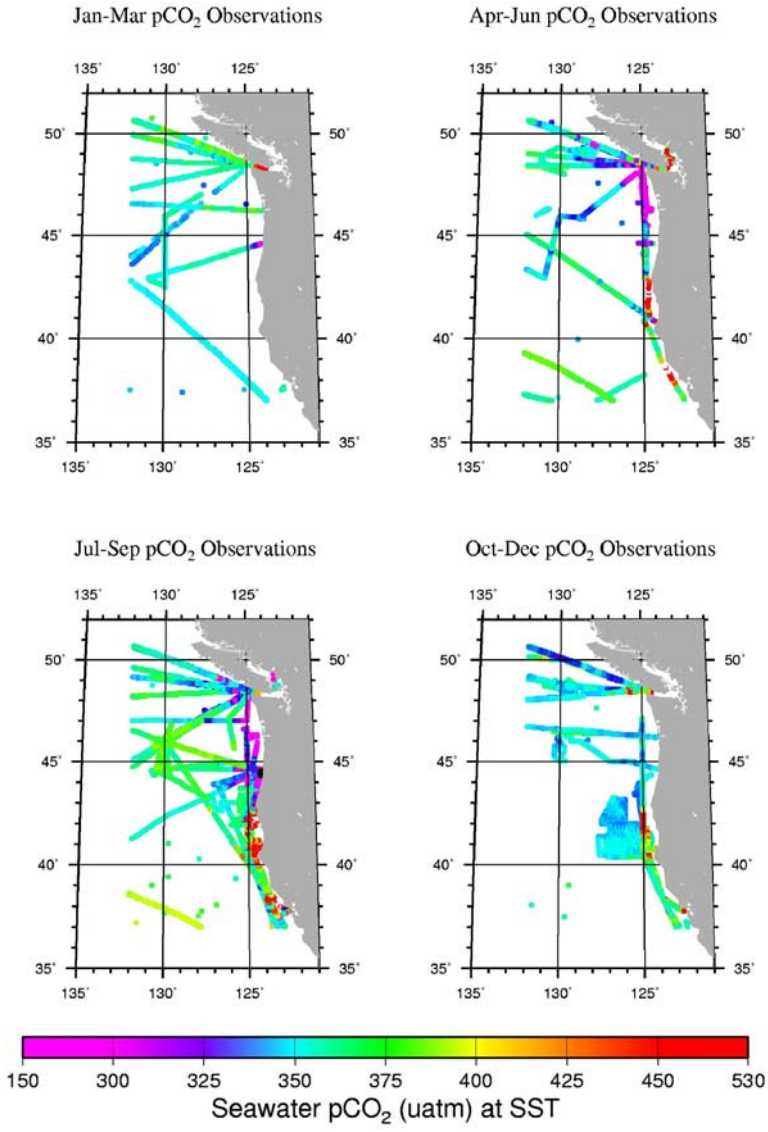

Figure 5. Composite of historical nearshore surface P_{CO2} measurements, corrected to a common year of 1995, collected aboard ships of opportunity. The color scale is for surface-water P_{CO2} in micro-atmospheres. The dark blue and magenta colors indicate a CO_2 sink area with low P_{CO2} values. The difference between P_{CO2} and X_{CO2} is less than a percent.

[8] This pattern persists in space and time. Surface water is undersaturated with respect to atmospheric CO_2 over most of the shelf, while supersaturated, freshly upwelled waters are seen at the surface only in narrow bands near the coast throughout the range of the study from 44°15′N to 45°00′N and from 125.00°W to the shore (Figure 3a). A week-long time series at the northernmost site (Figure 3b) shows short-term temporal variability due to upwelling-intensity fluctuations, with highest nearshore X_{CO2} seen during intense upwelling on 22, 26, and 27 May, and lower levels seen during relaxation (decreased equatorward wind intensity) during 24 and 25 May. Despite the large nearshore variability, seaward X_{CO2} remains remarkably constant at around 200 ppm.

[9] Longer timescale variability is assessed by comparing cross-shelf distributions in August (Figure 4) and May (Figure 2). Deep-water X_{CO2} (>1300 ppm) and T_{CO2} (an implied increase of 0.05 mmol kg^{-1}) are significantly higher in August due to local respiration, while surface waters remain at the low levels observed in May. Spatially and temporally weighted average surface ΔX_{CO2} is −130 ppm over the temporal and spatial scale of this study, implying a strong local seasonal sink for atmospheric CO_2.

[10] Other study of shelf-water CO_2 chemistry in this region has been limited. *Van Geen et al.* [2000], at a location a few hundred kilometers to the south, found a very similar dynamic range in surface-water X_{CO2} (150–690 ppm), and demonstrated the very-nearshore impacts of

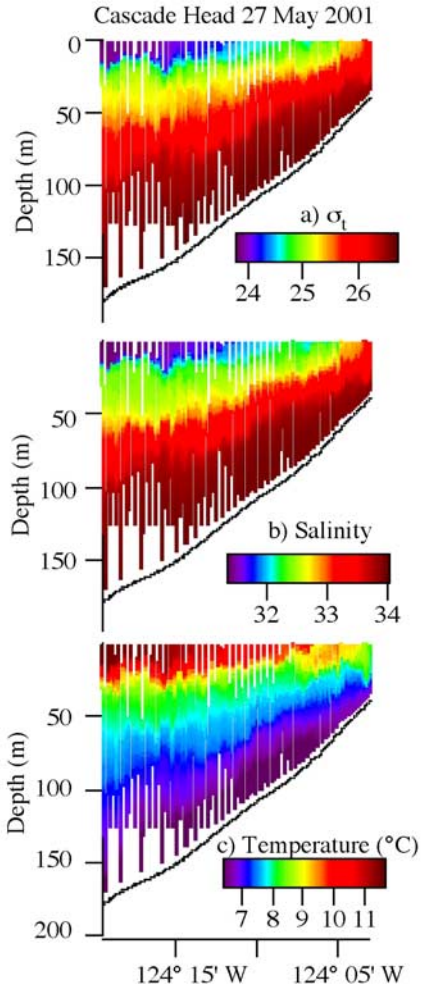

Figure 6. Cross-shelf sections of (a) density (expressed as density anomaly, sigma-t), (b) salinity, and (c) temperature at the Cascade head transect on 27 May 2001.

freshly upwelled water, but did not quantify spatially weighted average values. Composite seasonal historical surface ocean P_{CO2} distributions, collected during transits to and from port during large-scale open ocean CO_2 survey programs (Figure 5, unpublished results from the Global Ocean P_{CO2} Database at the Lamont-Doherty Earth Observatory (LDEO)) likewise show similar dynamic ranges, but the direct connections to upwelling processes were not made. Previous measurements thus corroborate our basic observations, but do not provide the detailed study of the connections between upwelling and productivity presented here, or quantify the impact on net air-sea CO_2 exchange.

4. Discussion

[11] The observation of persistent undersaturation of surface-water CO_2 with respect to the atmosphere in this coastal upwelling system prompts two immediate questions. First, what about this location differs from open-ocean upwelling areas, typically strong sources of CO_2 to the atmosphere? Second, is this sink significant in the global carbon budget?

4.1. Unique Biogeochemical Aspects of the Study Area

[12] In response to the first, we examined characteristics of the upwelled source water, which is easy to track at the northernmost site. Density anomaly (sigma-t; Figure 6, top panel) distributions show that dense water, with sigma-t $\geq$ 26.5, is drawn up and shoreward along the bottom. This water's salinity is nearly 34 (Figure 6, middle panel), and its temperature slightly less than 7°C (Figure 6, bottom panel). We chose to examine this water because it has been shown that the onshore upwelling transport originates primarily from this density range and proceeds onshore through the bottom boundary layer [e.g., *Smith*, 1974; *Lentz*, 1992; *Perlin et al.*, 2005].

[13] Reconstruction of the source water's CO_2 response to upwelling, warming, and photosynthesis requires some knowledge of its T_{CO2}. Temperature, salinity, and T_{CO2} profiles show that the source water's depth is about 200 m; T_{CO2}, measured by a discrete-sample modification of the continuous method of L. Bandstra et al. (High-frequency measurements of total CO_2: Method development and first oceanographic observations, submitted to *Marine Chemistry*, 2004), at this depth is 2.30 mmol kg^{-1} (Figure 7). This, and an observed source-water X_{CO2} of 975 ppm, allows calculation of a "pseudo-alkalinity" or a "calculated alkalinity" of 2.33 meq kg^{-1}. This calculation is based on acid-base equilibrium relationships and a simple model of alkalinity consisting of carbonate, bicarbonate, and borate ion concentrations (= $[HCO_3^-]$ + $2[CO_3^{-2}]$ + $[H_2BO_3^{-1}]$). Such a simple model may include errors associated with neglecting other species such as silicate, phosphate, and hydroxyl ions. The computed values are probably accurate to better than ±0.5% for estimation of total alkalinity, sufficient for this exercise. Both T_{CO2} and alkalinity values are consistent with those seen in similar-T/S waters on the WOCE P17N line [*Lamb et al.*, 2002] (World Ocean Circulation Experiment, available at http://whpo.ucsd.edu/data/onetime/pacific/p17/p17n), lending confidence to the basic observations summarized above.

[14] We know from our own high-resolution measurements (Hales et al., submitted manuscript, 2004), and from historical data [*Kokkinakis and Wheeler*, 1987] (U.S. GLOBal Ocean ECosystems Dynamics North East Pacific program, available at http://globec.coas.oregonstate.edu/jg/serv/globec/nep) of nutrient chemistry in this area, that the nitrate concentration in this source water is about 34 μmol/kg and is drawn to zero by rapid photosynthesis. The N:C stoichiometry ratio of 16:106 for photosynthetic uptake [e.g., *Redfield et al.*, 1963] implies that a decrease of 7 units of T_{CO2} and a 1 unit increase in alkalinity results from each 1 unit of nitrate decrease. This results in a biologically modified source water with T_{CO2} = 2.05 mmol kg^{-1}(= 2.30−0.25 mmol kg^{-1}) and alkalinity = 2.33 meq kg^{-1}(= 2.30 + 0.03 meq kg^{-1}). From these we calculate X_{CO2} = 165 ppm at the source-water temperature of 7°C. Warming, significant in determining X_{CO2} of any water

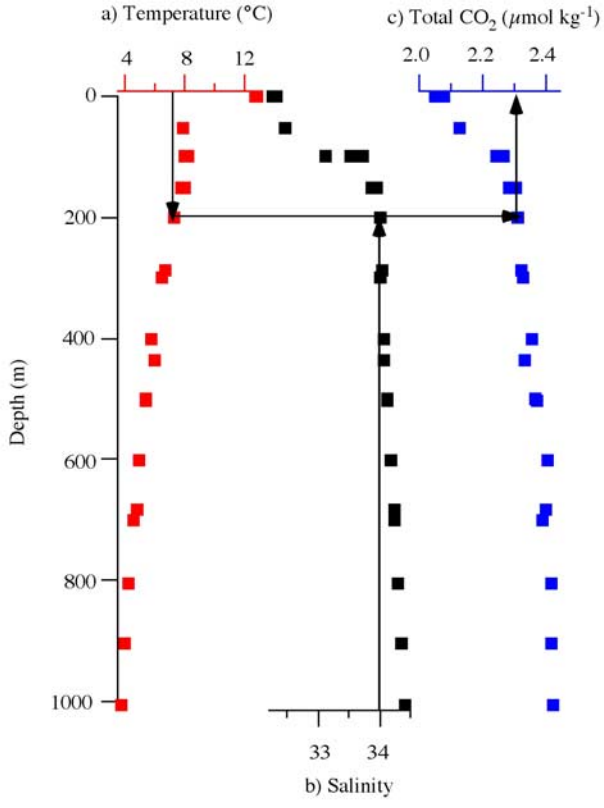

Figure 7. Vertical distributions of (a) temperature, (b) salinity, and (c) T_{CO2} at a 1000-m-deep station off Newport, Oregon. Arrows indicate the T, S, and corresponding T_{CO2} of the upwelled source water.

mass, raises temperatures to only 11° or 12°C, increasing X_{CO2} to only 215 ppm. These values are well within the range of surface X_{CO2} summarized in Figures 1–4.

[15] This exercise identifies several key aspects of this upwelling system. The first, and most significant, is the large preformed nutrient concentration of the upwelled source waters. The preformed nutrient concentration is the nutrient concentration at the time of the formation of water mass, and may be approximated by subtracting the respired amount from the observed concentration. The respired amount is commonly estimated using the apparent oxygen utilization (AOU) at the potential temperature and the respiration stoichiometry. Hence waters with large preformed nutrient values should support greater amounts of photosynthesis and yield low X_{CO2} waters when all the nutrients are utilized by the photosynthesis. Our own calibrated in situ O_2 data show a source-water O_2 concentration of 70 μmol kg^{-1}, corresponding to an apparent oxygen utilization (AOU) of 220 μmol kg^{-1}. On the basis of the AOU:NO_3^- respiration ratio [e.g., *Anderson and Sarmiento*, 1994; *Hedges et al.*, 2002; *Takahashi et al.*, 1985], we estimate that about 22 μmol kg^{-1} of the source-water NO_3^- was respiration-produced. The remaining 12 μmol kg^{-1} are preformed, consistent with the high NO_3^- of the 26.5 sigma-t surface outcrop in the western North Pacific in late winter [*Takahashi et al.*, 1993]. This will support an additional CO_2 utilization of 0.084 mmol kg^{-1}, when all the nutrients are consumed. This will reduce the X_{CO2} by an additional 50%.

[16] The second important aspect of this system is that productivity is limited only by available nitrate, evidenced by its complete exhaustion. There appears to be no micronutrient limitation, consistent with the upwelling path through the benthic boundary layer, which is exceptionally high in dissolved iron [*Chase et al.*, 2002]. There also appears to be no significant grazing limitation keeping primary producers from completely consuming available nitrate. The lack of limitation allows photosynthesizers to consume T_{CO2} in stoichiometric proportion to the total available nitrate.

[17] Finally, warming of these upwelled waters is modest in the study area. Water temperature increases by 4°–5°C across the shelf (Figure 6), which increases X_{CO2} by about 30% (50 ppm), which is much less than the reducing effect of the photosynthesis supported by preformed nutrients.

[18] All of these features contrast with the conditions experienced by, for example, the open-ocean upwelling region of the central and eastern equatorial Pacific. Upwelled water supplied to the euphotic zone there originates at the top of the Equatorial Undercurrent at a depth of ~100 m, and contains essentially no preformed nutrients [*Archer et al.*, 1996; *Chai et al.*, 1996; *Radenac and Rodier*, 1996]. Upwelled nutrients are not depleted to zero in surface waters [*Chai et al.*, 1996; *Murray et al.*, 1995; *Archer et al.*, 1996; *Radenac and Rodier*, 1996]. This implies a non-nutrient limitation of phytoplankton growth, either due to grazing [e.g., *Verity et al.*, 1996] or trace element limitation [e.g., *Fitzwater et al.*, 1996]. In addition, surface waters warm significantly, by nearly 10°C, as they move westward along the equator. These factors combine to make the equatorial Pacific one of the largest natural sources of CO_2 to the atmosphere [*Takahashi et al.*, 2002; *Tans et al.*, 1990].

4.2. Global Significance of the Upwelling Along the U. S. Pacific Coast

[19] To address the second question posed above, the net air-sea gas exchange flux (F) for the upwelling season must be quantified. F can be estimated from

$$F = -k_{CO_2} K_{CO_2} \Delta P_{CO_2},$$

where k_{CO2} is sea-air CO_2 gas transfer coefficient (m d^{-1}), K_{CO2} is CO_2 solubility (mol m^{-3} atm^{-1}), and ΔP_{CO2} is the sea-air P_{CO2} difference (atm). ΔP_{CO2} was calculated from the observed ΔX_{CO2}, ambient atmospheric pressure, and water-vapor content. The atmospheric pressure and water-vapor corrections are small (order a few percent each), and largely cancel each other; thus the ΔP_{CO2} values are nearly equivalent to the ΔX_{CO2} values presented earlier. To obtain the mean air-sea CO_2 flux for the study area and season, the mean values for each of the parameters in the equation above have been used. We determined a mean k_{CO2} for the May–August period by averaging k_{CO2} values calculated from wind speed measurements (hourly mean U_{10}; m s^{-1}) from the nearby NDBC buoy 46050 (National Data Buoy

Center; http://www.ndbc.noaa.gov) and the following dependence on U_{10} [*McGillis et al.*, 2001]:

$$k_{CO_2} = 0.79 + 0.0062U_{10}^3$$

[20] The average upwelling-season gas-exchange coefficient for CO_2, k_{CO2}, has been estimated to be 3 m d^{-1}. The mean flux was estimated by multiplying this mean k_{CO2} by the spatially and temporally weighted average ΔX_{CO2} given in section 3, corrected for atmospheric pressure and water-vapor content at the time of each surface CO_2 measurement. If correlation of ΔX_{CO2} with wind speed is weak, the season-average flux may be estimated from the product of the season-average k_{CO2} and our estimate of season-average ΔX_{CO2} given earlier. This assumption is supported by two observations. First, there is no correlation between wind speed and wind direction, as discussed earlier, arguing against any correlation between ΔX_{CO2} variability caused by upwelling/reversal cycles and k_{CO2}. Second, it has long been known that ΔX_{CO2} and wind velocity do not correlate strongly in the open ocean as a result of the strong buffering of ocean CO_2 with respect to gas exchange [e.g., *Broecker and Peng*, 1980]. We find that the average flux calculated in this way is 20 mmol m^{-2} d^{-1}, which is about 15 times as large as the mean global ocean CO_2 uptake flux of about 1.3 mmol m^{-2} d^{-1} (or 2 Pg-C yr^{-1}). If upwelling prevails May–August [*Allen et al.*, 1995; *Federiuk and Allen*, 1995; *Lentz*, 1992, *Strub et al.*, 1987a, 1987b], CO_2 uptake in this 120-day interval is 2 mol m^{-2}.

[21] This is a large area-specific flux, and the nearshore regions were specifically excluded from the global compilations such as that of *Takahashi et al.* [2002]. Assessing its global significance requires estimation of the area that such conditions cover. The limited number of studies of CO_2 chemistry in eastern boundary upwelling coastal waters makes such an extrapolation difficult at best. *Ianson and Allen* [2002] and *Ianson et al.* [2003], with a combination of modeling and measurements in the region immediately offshore of Vancouver Island at about 49°N, report a similar dynamic range to that reported here. Their reported X_{CO2} values range from 200 ppm to 1500 ppm, with the outer shelf representing a strong sink for atmospheric CO_2, and a narrow inner-shelf band representing a strong source. These findings are in good qualitative agreement with those presented here. *Friederich et al.* [2002], however, with a series of studies along a single cross-shelf transect off Monterey, California, concluded that that region represented a net source of CO_2 to the atmosphere. More recently, Friederich observed X_{CO2} variability along that transect consistent with that reported here, including some values as low as 150 ppm (G. Friederich, personal communication, 2004). Hydrographic data suggest that the water upwelled along the Oregon coast is present along the entire eastern boundary of the North Pacific [e.g., *Reid*, 1965; *Talley*, 1993]. If this water is supplied to the coastal ocean by upwelling along the entire margin, then it is possible that the conditions seen off Oregon are representative of a much greater area. The multiyear seasonal observations for the surface-water pCO_2 indicate that the low pCO_2 waters (dark blue and purple colors in Figure 5) are present during the spring-summer months as far west as 127°W or 235 km offshore (150 km west of the shelf break). We recognize that some other aspects of the Oregon coast system may not be general, for example, the complete and rapid photosynthetic uptake of excess nitrate and moderate warming of upwelled waters. These caveats must be taken into account when considering extrapolations of the sort we make below.

[22] Nonetheless, if the conditions seen off Oregon are representative, and if eastern-boundary upwelling regions in the North Pacific cover 0.7×10^6 km^2 (or 25% of the area of the contiguous Pacific shelf area with water depths between 0–200 m [*Menard and Smith*, 1966]), then upwelling-season uptake of atmospheric CO_2 by such areas is 2×10^{12} mol (0.02 Pg- C). Although this area represents less than 2% of the North Pacific 14°N–50°N, and the upwelling season lasts only a third of the year, the seasonal flux is about 5% of the mean annual North Pacific CO_2 uptake, estimated at about 40×10^{12} mol yr^{-1} (0.5 Pg C yr^{-1}) [*Takahashi et al.*, 2002; *Gloor et al.*, 2003]. Further, the uptake of CO_2 by this region is about half of the open North Pacific's CO_2 uptake during the same May–August period (www.ldeo.columbia.edu/CO2). These comparisons suggest that the sum of ocean margin upwelling systems, including the west coasts of North America, South America, and South Africa, could contribute significantly to the global air-to-sea CO_2 fluxes.

[23] The increased X_{CO2} of subsurface waters in the August sections of Figure 3 is caused by the respiration of locally produced biogenic debris settling through the water column, and hence is derived from photosynthetic production of organic carbon fueled by upwelled nutrients. Some portion of the atmospheric CO_2 taken up by the surface seawater over the shelf area is thus transferred to subsurface waters. During winter, poleward along-shore winds cause downwelling, which results in bulk subduction of the dense isopycnals that had been on the shelf during summertime [*Allen and Newberger*, 1996] to their $\geq$200 m offshore depths. This process would thus move high-CO_2 shelf water offshore to deep ocean-interior regimes, where the CO_2 could mix to even greater depths via enhanced vertical mixing along the continental slope [*Ledwell et al.*, 2000]. This represents an important pathway through which atmospheric CO_2 is sequestered in deep ocean regimes via a seasonal biological pump in shelf environments.

[24] Assessing the process of transfer of CO_2 to the ocean interior by the route suggested above requires observations during the fall transition from predominantly upwelling summer conditions to predominantly downwelling winter conditions to determine if impacted summertime waters are in fact moved offshore in bulk. We completed a series of studies in this region in January of 2003 (B. Hales unpublished results, 2003), and saw surface CO_2 values near or slightly below saturation with respect to the atmosphere. There was no indication of the presence of the dense upwelled waters seen in summer, and no hint of degassing from the respiration-driven high-P_{CO2} waters seen in the late summer data presented here. These observations thus tentatively support the notion of wholesale movement of CO_2-rich waters from the shelf to the ocean interior, but cannot definitively rule out offgassing processes in the fall transi-

tion period. Further field observations are required to determine the fate of the CO_2 sequestered during the summer upwelling season.

5. Conclusions

[25] High spatial resolution surveys of the CO_2 distributions in coastal ocean water off Oregon showed that the surface water in this area was a strong sink for atmospheric CO_2 during summer upwelling season. This sink is supported by complete photosynthetic uptake of respiration-derived and preformed nutrients in the waters upwelled in this region. Toward the end of the upwelling season, we observed that the TCO_2 concentration in near-bottom waters increased substantially due to the respiration of biogenic debris that settled through the water column. Respiration of photosynthetically produced matter exported from surface waters to depth results in a transfer of atmospheric CO_2 to deeper waters. Wintertime downwelling processes then move these waters en masse offshore and to depths of a few hundred meters, where the sequestered CO_2 can mix into the deep interior of the ocean. Because of the great lengths of the shorelines surrounding the continents, this pathway may play an important role in the global carbon cycle. Further observations are being made in order to assess its significance quantitatively.

[26] **Acknowledgments.** The authors are grateful to the Captain and crew of the RV *Thomas G Thompson* for their exceptional performance in executing the difficult multiple-instrument towing operation. J. Jennings' long history with continuous-flow chemical analyzers was a key factor in our next step forward in high-speed chemical analysis. P. Covert's development of automated data collection and system control was central to our ability to perform these operations continuously, around the clock. J. Goddard provided analyses of our standard gases to assure absolute CO_2 measurement accuracy. Thanks are owed to P. Wheeler, J. Allen, and J. Barth for providing leadership for the greater COAST program. This work was supported by NSF grant 9907854-OCE.

References

Allen, J. S., and P. A. Newberger (1996), Downwelling off the Oregon continental shelf: I. Response to idealized forcing, *J. Phys. Oceanogr.*, *26*, 2011–2035.

Allen, J. S., P. A. Newberger, and J. Federiuk (1995), Upwelling off the Oregon continental shelf: I. Response to idealized forcing, *J. Phys. Oceanogr.*, *25*, 1844–1866.

Anderson, L. A., and J. L. Sarmiento (1994), Redfield ratios of remineralization determined by nutrient data analysis, *Global Biogeochem. Cycles*, *8*, 65–80.

Archer, D. E., T. Takahashi, S. Sutherland, J. Goddard, D. Chipman, K. Rodgers, and H. Ogura (1996), Daily, seasonal, and interannual variability of sea-surface carbon and nutrient concentration in the equatorial Pacific Ocean, *Deep Sea Res., Part II*, *43*, 779–808.

Barth, J. A., S. D. Pierce, and R. L. Smith (2000), A separating coastal upwelling jet at Cape Blanco, Oregon and its connection to the California Current system, *Deep Sea Res., Part II*, *47*, 783–810.

Barth, J. A., T. J. Cowles, P. M. Kosro, R. K. Shearmann, A. Huyer, and R. L. Smith (2002), Injection of carbon from the shelf to offshore beneath the euphotic zone in the California Current, *J. Geophys. Res.*, *107*(C6), 3057, doi:10.1029/2001JC000956.

Broecker, W. S., and T.-H. Peng (1980), *Tracers in the Sea*, Lamont-Doherty Geol. Obs., Columbia Univ., Palisades, New York.

Chai, F., S. T. Lindley, and R. T. Barber (1996), Origin and maintenance of a high-nitrate condition in the equatorial Pacific, *Deep Sea Res., Part II*, *43*, 1031–1064.

Chase, Z., P. A. Wheeler, A. van Geen, P. M. Kosro, and J. Marra (2002), Iron, nutrient, and phytoplankton distributions in Oregon coastal waters, *J. Geophys. Res.*, *107*(C10), 3174, doi:10.1029/2001JC000987.

Chen, C.-T. A., A. Andreev, K.-R. Kim, and M. Yamamoto (2004), Roles of continental shelves and marginal seas in the biogeochemical cycles of the North Pacific Ocean, *J. Oceanogr.*, *60*, 17–44.

DeGrandpre, M. D., T. R. Hammar, G. J. Olbu, and C. M. Beatty (2002), Air-sea CO_2 fluxes on the US Middle Atlantic Bight, *Deep Sea Res., Part II*, *49*, 4355–4367.

Dugdale, R. C., E. P. Wilkerson, and A. Morel (1990), Realization of new production in coastal upwelling areas: A means to compare relative performance, *Limnol. Oceanogr.*, *35*, 822–829.

Federiuk, J., and J. S. Allen (1995), Upwelling off the Oregon continental shelf: II. Simulations and comparisons with observations, *J. Phys. Oceanogr.*, *25*, 1867–1889.

Fitzwater, S. E., K. H. Coale, R. M. Gordon, K. S. Johnson, and M. E. Ondrusek (1996), Iron deficiency and phytoplankton growth in the equatorial Pacific, *Deep Sea Res., Part II*, *43*, 995–1016.

Friederich, G. E., F. P. Chavez, P. M. Walz, and M. G. Burczynski (2002), Inorganic carbon in the central California upwelling system during the 1997–1999 El Niño–La Niña event, *Prog. Oceanogr.*, *54*, 185–203.

Gloor, M., R. A. Feely, C. Rodenbeck, N. Gruber, and J. Sarmiento (2003), A first estimate of present and pre-industrial air-sea CO_2 flux patterns based on ocean interior carbon measurements and models, *Geophys. Res. Lett.*, *30*(1), 1010, doi:10.1029/2002GL015594.

Hales, B., and T. Takahashi (2002), The Pumping Seasoar: A high resolution seawater sampling platform, *J. Oceanic Atmos. Technol.*, *19*, 1096–1104.

Hales, B., and T. Takahashi (2004), High-resolution biogeochemical investigation of the Ross Sea, Antarctica, during the AESOPS (U. S. JGOFS) Program, *Global Biogeochem. Cycles*, *18*, GB3006, doi:10.1029/2003GB002165.

Hales, B., T. Takahashi, and A. van Geen (2004a), High-frequency measurement of seawater chemistry: Flow-injection analysis of macronutrients, *Limnol. Oceanogr.*, *2*, 91–101.

Hales, B., T. Takahashi, and D. Chipman (2004b), High-frequency measurement of seawater dissolved inorganic carbon chemistry using microporous hydrophobic membrane contactors, *Limnol. Oceanogr.*, *2*, 356–364.

Hedges, J. I., C. Lee, M. L. Peterson, S. G. Wakeham, J. A. Baldock, and Y. Gélinas (2002), The biochemical and elemental compositions of marine plankton: A NMR perspective, *Mar. Chem.*, *78*, 47–63.

Huyer, A., R. Pillsbury, and R. Smith (1978), Seasonal variation of the alongshore velocity field over the continental shelf off Oregon, *Limnol. Oceanogr.*, *20*, 90–95.

Huyer, A., E. Sobey, and R. Smith (1979), The spring transition in currents over the Oregon continental shelf, *J Geophys. Res.*, *84*, 6995–7011.

Ianson, D., and S. E. Allen (2002), A two-dimensional nitrogen and carbon flux model in a coastal upwelling region, *Global Biogeochem. Cycles*, *16*(1), 1011, doi:10.1029/2001GB001451.

Ianson, D., S. E. Allen, S. L. Harris, K. J. Orians, D. E. Varela, and C. S. Wong (2003), The inorganic carbon system in the coastal upwelling region west of Vancouver Island, Canada, *Deep Sea Res., Part I*, *50*, 1023–1042.

Kokkinakis, S. A., and P. A. Wheeler (1987), Nitrogen uptake and phytoplankton growth in coastal upwelling regions, *Limnol. Oceanogr.*, *32*, 822–829.

Lamb, M. F., et al. (2002), Consistency and synthesis of Pacific Ocean CO_2 survey data, *Deep Sea Res., Part II*, *49*, 21–58.

Ledwell, J. R., E. T. Montgomery, K. L. Polzin, L. C. St. Laurent, R. W. Schmitt, and J. M. Toole (2000), Evidence for enhanced mixing over rough topography in the abyssal ocean, *Nature*, *403*, 179–182.

Lentz, S. J. (1992), The surface boundary layer in coastal upwelling regions, *J. Phys. Oceanogr.*, *22*, 1517–1539.

McGillis, W. R., et al. (2001), Carbon dioxide flux techniques performed during GasEx-98, *Mar. Chem.*, *75*, 267–280.

Menard, H. W., and S. M. Smith (1966), Hypsometry of the ocean basin provinces, *J. Geophys. Res.*, *71*, 4305–4325.

Murray, J. W., E. Johnson, and C. Garside (1995), A U.S. JGOFS process study in the Equatorial Pacific (EqPac): Introduction, *Deep Sea Res., Part II*, *42*, 275–294.

Perlin, A., J. N. Moum, and J. M. Klymak (2005), Response of the bottom boundary layer over a sloping shelf to variations in alongshore wind, *J. Geophys. Res.*, doi:10.1029/2004JC002500, in press.

Radenac, M.-H., and M. Rodier (1996), Nitrate and chlorophyll distributions in relation to thermohaline and current structures in the western tropical Pacific during 1985–1989, *Deep Sea Res., Part II*, *43*, 725–752.

Redfield, A. C., B. H. Ketchum, and F. A. Richards (1963), The influence of organisms on the composition of seawater, in *The Sea: Ideas and Observations on Progress in the Study of the Seas*, vol. 2, edited by M. N. Hill, pp. 26–77, John Wiley, New York.

Reid, J. L., Jr. (1965), Intermediate waters of the Pacific Ocean, *Johns Hopkins Oceanogr. Stud.*, *2*, 85 pp.

Smith, R. L. (1974), A description of current, wind and sea level variations during coastal upwelling off the Oregon coast, July–August 1972, *J. Geophys. Res.*, *79*, 435–443.

Strub, P. T., J. S. Allen, A. Huyer, and R. Smith (1987a), Large-scale structure of the spring transition in the coastal ocean off western North America, *J. Geophys. Res.*, *92*, 1527–1544.

Strub, P. T., J. S. Allen, A. Huyer, R. Smith, and R. Beardsley (1987b), Seasonal cycles of currents, temperatures, winds, and sea level over the Northeast Pacific continental shelf, *J. Geophys. Res.*, *92*, 1507–1526.

Takahashi, T., W. S. Broecker, and S. Langer (1985), Redfield ratio based on chemical data from isopycnal surfaces, *J. Geophys. Res.*, *90*, 6907–6924.

Takahashi, T., J. Olafsson, J. G. Goddard, D. W. Chipman, and S. C. Sutherland (1993), Seasonal variation of CO_2 and nutrients in the high-latitude surface oceans: A comparative study, *Global Biogeochem. Cycles*, *7*, 843–878.

Takahashi, T., et al. (2002), Global air-sea CO_2 flux based on climatological surface ocean pCO_2 and seasonal biological and temperature effects, *Deep Sea Res., Part II*, *49*, 1601–1622.

Talley, L. (1993), Distribution and formation of North Pacific Intermediate Water, *J. Phys. Oceanogr.*, *23*, 517–537.

Tans, P. P., I. Y. Fung, and T. Takahashi (1990), Observational constraints on the global atmospheric CO_2 budget, *Science*, *247*, 1431–1438.

Thomas, H., Y. Bozec, K. Elkalay, and H. J. W. de Baar (2004), Enhanced open ocean storage of CO_2 from shelf sea pumping, *Science*, *304*, 1005–1008.

Tsunogai, S., S. Watanabe, and T. Sato (1999), Is there a "continental shelf pump" for the absorption of atmospheric CO_2?, *Tellus, Ser. B*, *51*, 701–712.

van Geen, A., R. K. Takesue, J. Goddard, T. Takahashi, J. A. Barth, and R. L. Smith (2000), Carbon and nutrient dynamics during coastal upwelling off Cape Blanco, Oregon, *Deep Sea Res., Part II*, *47*, 975–1002.

Verity, P. G., D. K. Stoecker, M. E. Sieracki, and J. R. Nelson (1996), Microzooplankton grazing of primary production in the equatorial Pacific, *Deep Sea Res., Part II*, *43*, 1227–1256.

Yool, A., and M. J. R. Fasham (2001), An examination of the "continental shelf pump" in an open ocean general circulation model, *Global Biogeochem. Cycles*, *15*, 831–844.

L. Bandstra and B. Hales, College of Oceanic and Atmospheric Sciences, Oregon State University, 104 Ocean Administration Building, Corvallis, OR 97331, USA. (bhales@coas.oregonstate.edu)

T. Takahashi, Lamont-Doherty Earth Observatory of Columbia University, Palisades, NY 10964, USA.